

High Accuracy OH Reaction Rate Constants of CH₂=CF-CF₃ and *trans*-CHF=CF-CF₃ and IR Absorption Spectra.

Vladimir L. Orkin^{*}, Larissa E. Martynova, and Alexander N. Ilichev^a

Physical and Chemical Properties Division,
National Institute of Standards and Technology,
Gaithersburg, Maryland 20899

Abstract

Rate constants for the gas phase reactions of OH radicals with two isomers of tetrafluoropropene, CH₂=CF-CF₃ (*k*₁) and *trans*-CHF=CH-CF₃ (*k*₂); were measured using a flash photolysis resonance-fluorescence technique over the temperature range 220 K to 370 K. The Arrhenius plots were found to exhibit a noticeable curvature. The temperature dependences of the rate constants are very weak and can be represented by the following expressions over the indicated temperature intervals:

$$k_1(220 - 298 \text{ K}) = 1.146 \times 10^{-13} \times \exp\{-13/T\} \text{ cm}^3 \text{ molecule}^{-1} \text{ s}^{-1}$$

$$k_1(298 - 370 \text{ K}) = 1.49 \times 10^{-13} \times \exp\{-92/T\} \text{ cm}^3 \text{ molecule}^{-1} \text{ s}^{-1}$$

$$k_2(220 - 370 \text{ K}) = 1.11 \times 10^{-13} \times (T / 298)^{2.03} \times \exp\{+554/T\} \text{ cm}^3 \text{ molecule}^{-1} \text{ s}^{-1}$$

The atmospheric lifetimes due to reactions with tropospheric OH were estimated to be 12 and 19 days respectively under assumption of the well mixed atmosphere. IR absorption cross-sections were measured for both compounds and their global warming potentials were estimated.

^a Present address: Semenov Institute of Chemical Physics, Russian Academy of Sciences, Kosygin str. 4, 119991 Moscow.

Introduction.

The internationally legislated elimination of chlorofluorocarbons (CFCs) from industrial applications, due to the established danger that they pose to Earth's ozone layer, has stimulated considerable study of the atmospheric properties of possible chemical substitutes. Chlorine free partially fluorinated hydrocarbons (hydrofluorocarbons or HFCs) were among the leading environmentally acceptable CFC alternatives from the point of view of ozone depletion. They replaced CFCs in industrial applications with HFC-134a being the most widely known example. However the rising concern about the possible impact of industrial chemicals on Earth's climate and possible tightening nation and international regulations stimulate the further search of environmentally acceptable compounds. Fluorinated alkenes are currently under consideration as potential environmentally friendly CFC substitutes. The presence of a carbon-carbon double bond is expected to render these substances highly reactive towards the hydroxyl radical, OH, resulting in an extremely short tropospheric lifetime, thereby limiting their accumulation in the atmosphere. This should minimize the global environmental impact including the warming of the atmosphere. Quantification of the possible role of new compounds as "greenhouse gases" requires accurate information on their atmospheric lifetimes, which are key parameters in determining the environmental consequences following their release into the atmosphere. These data when combined with IR absorption spectra of the compound allow the estimations of global warming potentials (GWP) through either semi-empirical estimations or thorough radiative-transfer modeling. In order to quantify the atmospheric lifetimes and GWPs, we have investigated the reactivity towards OH of two isomers of tetrafluoropropenes, 2,3,3,3-tetrafluoropropene and trans-1,3,3,3-tetrafluoropropene:



The quantitative results of their IR absorption cross-sections measurements are also reported.

The first reaction has the long history of studies in our laboratory. It was originally studied a decade ago under complicated conditions when $\text{CH}_2=\text{CFCF}_3$ was available as an impurity in the sample of HFC-245fa ($\text{CH}_3\text{CF}_2\text{CF}_3$).¹ Later we studied a pure sample of the compound provided by *Honeywell International Inc.* Finally we completed the study of this reaction by using our recently renewed flash photolysis-resonance fluorescence apparatus. This allows us to better estimate the actual instrumental uncertainties associated with OH reaction rate constant measurements. The OH reactivity of the second molecules, *trans*- $\text{CHF}=\text{CHCF}_3$ was also investigated twice by using our apparatus before and after modification. Meanwhile three papers devoted to the study of photochemical parameters of these molecules appeared recently^{2,3,4} allowing accurate evaluation of these parameters.

Thus the purpose of this paper is to provide accurate photochemical parameters for two compounds of potential industrial interest and, at the same time, to illustrate a possibility of OH reaction rate constant determinations with the accuracy as small as 2-3%.

Experimental Section⁵

OH Reaction Rate Constants Measurements.

The general descriptions of the apparatus and the experimental method used to measure the OH reaction rate constants are given in previous papers.^{6,7,8} In the present work we used the same principal configuration of the apparatus with a number of modifications made to improve the accuracy of the obtained kinetic data by decreasing and quantifying the instrumental uncertainties associated with measurements. In particular, the gas handling system was completely replaced, the new reaction cell, and new photomultiplier were used. The brief description followed by the uncertainty analysis is given here. The principal component of the flash photolysis-resonance fluorescence apparatus is a Pyrex reactor (of approximately 180 cm³ internal

volume) thermostated with methanol or water circulated through its outer jacket. This double-wall reactor is located in the metal vacuum housing evacuated to prevent the ambient water condensation during low temperature measurements. It also prevents the absorption of the UV radiation from a flash lamp which is used to produce OH radicals. Reactions were studied in argon carrier gas (99.9999% or 99.9995 % purity) at a total pressure of 4.00 kPa to 40.00 kPa (30.0 Torr to 300.0 Torr). Flows of dry argon, argon bubbled through water thermostated at 276 K, and fluoropropene mixtures (containing 0.1% to 100% of the reactant) flowed through the reactor at a total flow rate between 0.3 and 2.5 cm³ s⁻¹, STP. The fluoropropene mixtures diluted with argon were premixed in glass bulbs (2 L, 5 L or 10 L) equipped with Teflon/glass valves (J. Young Scientific Glassware). The concentrations of the gases in the reactor were determined by measuring the gas flow rates and the total pressure with MKS Baratron manometers. Flow rates of argon, H₂O/argon mixture, and the reactant/argon mixture were maintained and measured using MKS mass flow controllers directly calibrated for each mixture.

Hydroxyl radicals were produced by the pulsed photolysis (0.6 – 2.5 Hz repetition rate) of H₂O, injected via the 276 K argon/water bubbler. The use of the below room temperature water bubbler assures the smaller and more stable concentration of water vapor in the reactor. The OH radicals were monitored by their resonance fluorescence near 308 nm, excited by a microwave-discharge resonance lamp (440 Pa or 3.3 Torr of a ca. 2 % mixture of H₂O in UHP helium) focused into the reactor center. Resonantly scattered radiation from the center of the reaction cell was collimated by the reactor window-lens and detected by a cooled photomultiplier working in the photon counting mode. The photomultiplier operation parameters were chosen so that photon counting obeys statistics. The resonance fluorescence signal was recorded on a computer-based multichannel scanner (channel width 100 μs) as a summation of 500 to 5,000 consecutive flashes. Therefore the entire temporal OH profile was recorded and co-added following each flash thus

naturally accounting for possible small flash-to-flash variations of the initial OH concentration. The OH decay signal at each reactant concentration was analyzed as described by Orkin *et al.*⁷ to obtain the first-order decay rate coefficient due to the reaction under study.

The fluoropropene concentration ranged from ca. 7×10^{12} to 6×10^{14} molecule/cm³ in our experiments. At each temperature the rate constant was determined from the slope of a plot of the decay rate versus the reactant concentration. The measured [OH] decay rate due to the reaction with fluoropropenes ranged from ca. 6 s^{-1} to ca. 430 s^{-1} in our experiments. One potential source of the systematic uncertainty in such experiments is the change of the background OH decay – the variation of the measured OH decay rate in the absence of the reactant (fluoropropene) in the reactor. This “background” decay was usually recorded before and after a series of measurements at different reactant concentrations. It was very stable under the normal operation conditions, usually better than 0.5 s^{-1} during runs of many hours. This is one of the advantages of using a non-reactive OH precursor, H₂O. The temperature points for the measurements were chosen to be approximately equally distant along the Arrhenius $1/T$ scale in order to have them properly (i.e., equally) weighted in the following fitting procedure. In particular, experiments were performed at the two temperatures that are widely used in other studies, $T = 298 \text{ K}$ and $T = 272 \text{ K}$. The first one is the standard temperature used in the evaluations and presentations of the rate constants while the second one is the temperature used in estimations of the atmospheric lifetime⁹. In order to check for any complications, test experiments were performed with the following variations of experimental parameters: the total pressure in the reactor (between 30 Torr and 300 Torr), the H₂O concentration (a factor of 4), the flash energy (a factor of 4), the flash repetition rate (a factor of 4, between 0.6 and 2.5 Hz), the residence time of the mixture in the reactor (a factor of 8), and the reactant concentration in the storage bulb (a factor of 100).

IR Absorption Cross-Sections Measurements.

The IR absorption spectra were measured by using FTIR spectrophotometer *Nicolet 6700* with a spectral resolution of ca. 0.125 cm^{-1} (recorded with a step of ca. 0.06 cm^{-1}) and 0.5 cm^{-1} (recorded with a step of ca. 0.25 cm^{-1}). The test experiments were performed with a spectral resolutions of 0.25 cm^{-1} , and 1 cm^{-1} . All the IR absorption data presented in this paper were obtained by using a deuterated-triglycine-sulfate detector (DTGS) operated at near room temperature. A liquid nitrogen cooled mercury-cadmium-tellurium detector (MCT) was also used for test measurements. While a MCT detector is much faster and more sensitive than DTGS, the second one is characterized by better linearity and larger dynamic range. In addition the spectral range of a DTGS detector extends to longer wavelengths. However, the most important is that the data obtained with an ambient temperature detector, DTGS, are free of FT-IR instrumental artifacts which can affect the results of measurements with a cold detector at longer wavelengths. These problems can be pronounced at longer wavelengths when a low temperature MCT detector is used to obtain the higher resolution spectra.^{10,11,12} In this case the small aperture's iris works like a non-collimated additional source of radiation for a cold detector. The presence of such artifact can be visualized when FT-IR apparatus "shows" the presence of radiation over the wavelength region which is well beyond the optics transmission region (at wavenumbers smaller than 400 cm^{-1} in the case of KBr optics). This may result in the overestimation of the determined absorption cross sections when MCT detector is used. We found this effect to be moderate for measurements with 0.5 cm^{-1} spectral resolution when larger aperture can be used. It became very pronounced when data were collected with better spectral resolution of 0.125 cm^{-1} . Therefore we used only DTGS detector and Boxcar apodization to obtain the data presented in this paper. The data were recorded with 32 – 128 scans. The photometric noise was as low as 0.0003 absorption units at larger wavenumbers (1000 cm^{-1} – 2000 cm^{-1}) and increased up to ca. 0.003 absorption units at smaller wavenumbers (600 cm^{-1}).

The (10.2 ± 0.05) cm glass absorption cell fitted with KBr windows was fixed in the spectrophotometer to minimize a baseline shift. The temperature of the cell was $T = (295 \pm 1)$ K. Between measurements the cell was pumped out down to ca. 0.01 Pa and then filled with the gas to be studied. Absorption spectra of the evacuated cell and of the cell filled with a gas sample were alternately recorded several times, and the absorption cross sections at the wavenumber ν (cm^{-1}) were calculated as

$$\sigma(\nu) = \frac{2.303}{[TFP] \times L} \times (A_{TFP}(\nu) - A_0(\nu)) \quad (3)$$

where $\sigma(\nu)$ is the absorption cross-section at wavenumber ν , in units of $\text{cm}^2 \text{ molecule}^{-1}$; $A_{TFP}(\nu)$ and $A_0(\nu)$ are absorbancies (base 10) in the presence of tetrafluoropropene and of the evacuated cell at wavenumber ν , respectively; $[TFP]$ is the concentration of tetrafluoropropene, in units of $\text{molecule}/\text{cm}^3$; and L is the optical path length in cm. Measurements were performed at various pressures of a compound to verify adherence to the Beer-Lambert absorption law and obtain strong and weak absorption features of the spectrum. The final absorption spectra presented here were constructed from the results of individual measurements over the range of pressures; the original data obtained with the absorbancies between 0.3 and 0.8 were used. Thus the final spectra were constructed from the data points which obey the Beer-Lambert law and measured at reasonably high signal-to-noise ratios. The overall instrumental error associated with the optical path length, pressure measurements, temperature stability, and measured absorbance was estimated to be less than 2% for the strong measured absorption bands.

Pressure Measurements. Two MKS Baratron manometers (100 Torr full scale and 1000 Torr full scale) were used to measure and control the pressure in the reactor. These manometers controlled a downstream valve to maintain the reactor pressure to better than ca. ± 0.05 Torr (7 Pa). Two MKS manometers, 100 Torr

(13.33 kPa) and 1000 Torr (133.3 kPa) were used to prepare the reactant mixtures. The majority of measurements were performed with 1% mixture of $\text{CH}_2=\text{CFCF}_3$ and 1.5% mixture of $\text{CHF}=\text{CFCF}_3$ in Ar. In addition the 0.1%, 0.3%, 3%, 10%, and 100% mixtures were used for a number of test experiments. Two MKS manometers, 10 Torr (1.33 kPa) and 1000 Torr (133.3 kPa) were used to control the pressure in the absorption cell when IR absorption spectra were measured. All these manometers were adjusted and inter-calibrated by using the “laboratory pressure standard” – MKS Type 690A Baratron manometer with the MKS stated accuracy of 0.08%. This later manometer was directly calibrated using the NIST Primary Pressure Standard with the total uncertainty of less than 0.05% and was carefully handled after calibration. We conservatively accept the total relative uncertainty of pressure measurements to be 0.1% for our kinetic experiments.

Temperature. The temperature in the reactor center (geometrical intersection of all three optical axes: the flash lamp radiation, the radiation from the detection resonance discharge lamp, and the view of a photomultiplier) was calibrated by using 0.08 mm bare T-type (Copper/Constantan) thermocouples. The temperature of incoming and outgoing liquid was measured along with the temperature in the reaction center and the temperature distribution in its vicinity at our “standard” temperatures between 220 K and 370 K (220, 230, 250, 272, 298, 330, and 370 K). In the real kinetic experiments there was no thermocouple in the reactor center and the temperature was determined from these calibrations based on measured temperatures of both incoming and outgoing liquid which required a few tenths of degree corrections. Thermocouples were calibrated to be accurate to within 0.1 C at 0 C (melting ice) and 0.3 C at 100 C (boiling water). This uncertainty can gradually increase up to 1 C at the lowest temperature $T = 220$ K of our experiments.¹³ The spatial distribution of the temperature around the reactor center was also measured at all temperatures. The characteristic size of the detection zone in the reactor was less than 0.7 cm. The temperature deviation at ca.

0.5 cm and 1 cm off-center was ca. ± 0.1 K and ± 0.2 K at the highest temperature (370 K) and ca. ± 0.2 K and ± 0.4 K at the lowest one (220 K), respectively. Note that the relative error which can be introduced by the gas temperature uncertainty and/or fluctuations during the long experiments is offset to some extent by the opposite temperature dependencies of the reactant concentration and the measured rate constant.¹⁴

Flow rate measurements. All mass flow controllers were directly calibrated for every mixture by measuring the rate of pressure change in the same volume – the reaction cell isolated from the vacuum pump by using the same reaction cell manometer. (An additional volume was connected to the reactor for larger flow rates of argon carrier gas.) The temperature of the cell was maintained equal to the ambient laboratory temperature (± 0.2 C) to have the entire calibration volume (the jacketed reactor with non-jacketed connecting tubes) at the same temperature. The measured rates of the pressure change in the reactor were then normalized to $T = 298$ K, to have all the flow calibration finally obtained at the same temperature with the same volume. The statistical uncertainty of such calibrations is usually within 0.1% - 0.2% for argon diluted mixtures with the uncertainty larger than 0.2% being indicative of a relatively poor calibration in the present experiment. This uncertainty increases to 0.5 – 1% for pure non-diluted reactants. There is an obvious reason for this larger uncertainty – the actual gas flow rate of a pure compound is much smaller than for argon diluted mixtures at the same settings of a flow controller which resulted in much longer measurements. The determination of the reactant concentration in the reactor requires only the absolute pressure in the reactor and relative gas flow rates. Therefore, this calibration procedure allows us to minimize the related instrumental uncertainty of the measurements. Results of our calibrations are in very reasonable agreement with the factory stated accuracy of mass flow controllers, 0.2% to 0.3%. The flow controllers allowed variation of the flow rate by a factor of 100. However, there are optimal experimental conditions to minimize the uncertainties associated with gas handling and provide the appropriate range of

the reaction concentrations in the reactor. The majority of our measurements were performed at 4.00 kPa (30.0 Torr) and the total gas flow rate of $1.3 \text{ cm}^3\text{s}^{-1}$, STP. The test experiments were performed to check for the possible dependence of the measured reaction rate constant upon flow parameters.

Reactant concentration in the mixture. We used the reactants (fluoropropenes) premixed with argon in a 5 L glass bulbs to feed a corresponding MKS flow controller. The mixtures were carefully prepared manometrically in 5 L glass bulbs with the attention paid to their thermal equilibration during the mixing. The most suitable concentrations to run flow controllers under the optimum conditions in our experiments were 1% for $\text{CH}_2=\text{CFCF}_3$ and 1.5% for $\text{CHF}=\text{CFCF}_3$. The accuracy of the mixture preparation depends on the precision of manometers reading (less than 0.2%) and the ambient temperature fluctuation (drift) during the mixing (less than 0.5 K). Thus the uncertainty associated with the mixing itself should not exceed ca. 0.4%. The most uncertain factor is a potential possibility of the reactant absorption (or desorption) from the mixture during the storage in a bulb or when flowing through the gas handling system and the reaction cell. The reactant concentration in a storage bulb was checked by using IR absorption to find no measurable discrepancy between the content of the manometrically prepared mixtures and their IR analyses which was accurate to ca. 0.5%. The test kinetic measurements were performed at various (a factor of eight) total gas flow through the gas handling system and the reaction cell. Also the test experiments were performed with very different reactant concentrations in the storage bulb – both an order of magnitude larger and smaller than the optimal concentration used for the majority of measurements.

Based on the above analysis we can estimate the systematic instrumental uncertainty associated with all really accountable sources of uncertainty. The following is a summary of these sources with associated conservative relative uncertainties. 1. Preparation of the reactant mixtures in the storage bulbs: two pressure

measurements (0.2% each) and the temperature stability of the bulb (0.3%). 2. Pressure in the kinetic reactor: absolute pressure measurements (0.2%) and pressure fluctuations during the experiment (0.2%). 3. Flow controllers: Ar carrier gas flow (0.3%) and reactant mixture flow (0.3%). 4. Temperature of the reacting gas mixture in the photolysis/detection region: 0.05% at 298 K, 0.1% at 370 K, and 0.5% at 220 K. Combining these uncertainties as a doubled square-root of the sum of squares we can estimate the total uncertainty as ca. 1.5% increasing to 2% at the lowest temperature of our experiments, 220 K. This is the conservative value of the total uncertainty associated with gas handling in our experiments which can be estimated strictly based on the estimated individual uncertainties. It should be added to the calculated “statistical” uncertainty - two standard errors from the least-squares analysis of the data scattering in the OH kinetic experiments. Any additional potential experimental errors associated with secondary chemistry or reactant absorption/desorption should be checked, revealed and either eliminated or estimated and added to the uncertainty.

Materials. The high purity samples of tetrafluoropropenes were provided by *Honeywell International*. We studied two samples of trans-1,3,3,3-tetrafluoropropene ($\text{CHF}=\text{CHCF}_3$) with 99.92% and 99.99% purity. The only detected impurity in both samples was 3,3,3-trifluoro-1-propyne ($\text{CH}\equiv\text{CCF}_3$) in the amount of 0.08% and 0.01% respectively. The sample of 2,3,3,3-tetrafluoropropene ($\text{CH}_2=\text{CFCF}_3$) was ca. 99.9% purity with ca. 0.1% impurity of 3,3,3-trifluoropropene ($\text{CH}_2=\text{CHCF}_3$). These samples were used as is without any further purification except degassing. We used 99.9995% and 99.9999% purity argon (*Spectra Gases Inc.*) as a carrier gas.

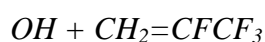
Results and Discussion

OH reaction rate constants.

The rate constants determined for the title reactions are presented in Tables 1 and 2. The bold-highlighted data are the fit results to all measurements performed at the particular temperature and 30.0 Torr total pressure. These data were obtained with 1% ($\text{CH}_2=\text{CFCF}_3$) and 1.5% ($\text{CHF}=\text{CHCF}_3$) mixtures prepared in the storage bulbs. These particular mixtures were chosen simply because they were convenient to maintain the appropriate reactant concentrations in the reaction cell with our apparatus design. The bold highlighted results are shown in Figures 1 and 2 along with other available data for these reactions. These figures show that both rate constants have very slow temperature dependence: the variation of the rate constants for both reactions over the entire temperature range is about 8% only. Therefore, the analysis of the obtained results is also of methodological interest illustrating the abilities for precise measurements of OH reaction rate constants. Arrhenius plots for these reactions exhibit curvature which is clearly resolved by our measurements.

Some results of test experiments are also shown in these tables. The “technical” test experiments were performed to check possible instrumental error which could increase the uncertainty of our results. The italicized results in Tables are indicative for the absence of any effect of gas flow rate (the residence time of the mixture in the system) on the measured rate constants. The variation of the reactant concentration in the storage bulbs by two orders of magnitude had no effect either. In addition, the quantitative IR analysis of the mixtures in the storage bulbs confirmed the content of manometrically prepared mixtures with the reactants concentrations as large as 10% and as small as 0.1%. We used the middle range concentrations of ca. 1% in our experiments. Thus, there was no indication of any additional systematic uncertainty in the reactant concentrations found other than those associating with pressure, temperature and flow rate measurements discussed above.

A few additional experiments were done to check for possible kinetic complications. In both reactions under study OH radicals disappear through the addition reaction. Therefore, in spite of multi-atomic nature of unsaturated molecules of reactants there is an illusive possibility that these reactions are pressure dependent. The test experiments revealed no indication of possible increase of the rate constants when pressure was increase by an order of magnitude. Therefore, the reaction rate constants presented in this paper are free of experimental or kinetic artifacts and characterize the title elementary chemical reactions.



A three-parameter modified Arrhenius dependence can be fit to the data set bold highlighted in Table 1 to result in the following expression:

$$k_1(220 - 370 \text{ K}) = 5.50 \times 10^{-13} \times (T / 298)^{0.866} \times \exp\{+207/T\}, \text{ cm}^3 \text{ molecule}^{-1} \text{ s}^{-1} \quad (4)$$

This dependence is shown in Figure 1 with the dashed line. In spite of very good fit to the individual points, one can see that this dependence probably does not reflect the trend especially at below room temperatures of atmospheric interest. Therefore, we suggest a simple Arrhenius dependence which was obtained from the fit to the data at $T < 298 \text{ K}$ and shown in Figure 1 with the solid line:

$$k_1(220 - 298 \text{ K}) = (1.146 \pm 0.012) \times 10^{-13} \times \exp\{-(13 \pm 3)/T\}, \text{ cm}^3 \text{ molecule}^{-1} \text{ s}^{-1} \quad (5)$$

The uncertainties indicated here and everywhere in the text are two standard errors obtained from the statistical least-squares fit unless stated otherwise. Note that both this dependence and the original data from Table 1 give the variation of the reaction rate constant over the entire range of atmospheric interest of ca. 1.5% only. Thus the average value is $k_1(220 - 298 \text{ K}) = (1.09 \pm 0.02) \times 10^{-12}$, $\text{cm}^3 \text{ molecule}^{-1} \text{ s}^{-1}$ with the error bars encompassing all the data obtained between 298 K and 220 K with their statistical uncertainties. The above room temperature data can be represented by the following expression:

$$k_1(298 - 370 \text{ K}) = (1.49 \pm 0.07) \times 10^{-13} \times \exp\{-(92 \pm 16)/T\}, \text{ cm}^3 \text{ molecule}^{-1} \text{ s}^{-1} \quad (6)$$

The only detected impurity in the samples of CH₂=CF₂CF₃ was 3,3,3-trifluoropropene. The reaction between OH and CH₂=CHCF₃ is only about 50% faster than reaction (1) under study.¹⁵ Therefore ca. 0.1% impurity of CH₂=CHCF₃ cannot affect the measured value of k_1 .

There are published results of three studies available for this reaction. A decade ago we determined its rate constant of this reaction with no pure sample available:¹⁵ CH₂=CF₂CF₃ has been found as ca. 6% impurity in the sample of HFC-245cb (CH₂FCH₂CF₃). The disappearance of OH in that mixture of CH₂=CF₂CF₃ with CH₂FCH₂CF₃ was mainly due to reaction (1) because of two orders of magnitude difference in their reactivity toward OH.¹⁵ The main complication was the quantitative determination of the concentration of CH₂=CF₂CF₃ in that mixture. It was done by employing the photochemical titration of CH₂=CF₂CF₃ by molecular bromine followed by the quantitative photometric measurements of Br₂ concentration. The results are shown in Figure 1 with open circles. Surprisingly even for us, these data coincide with the results of our present most accurate measurements to better than 2%. Moreover, the temperature dependence derived from those data,¹⁵ $k_1(252-370\text{ K}) = (1.41 \pm 0.12) \times 10^{-12} \times \exp\{-(64 \pm 27)/T\}$, cm³ molecule⁻¹ s⁻¹, coincide with an Arrhenius expression which could be derived from the fit to the present data between 250 K and 370 K, $k_1(250-370\text{ K}) = (1.31 \pm 0.12) \times 10^{-12} \times \exp\{-(50 \pm 22)/T\}$, cm³ molecule⁻¹ s⁻¹. Along with this curious results there are two recent publications on this reaction. Nielson *et al.*¹⁶ reported $k_1(296\text{ K}) = (1.05 \pm 0.17) \times 10^{-12}$, cm³ molecule⁻¹ s⁻¹ determined by a relative rate technique. This value coincides with our results and is shown as a triangle in Figure 1. Papadimitriou *et al.*⁴ reported k_1 obtained between 207 K and 380 K which are shown as squares in Figure 1. Authors reported the overall uncertainty of their data as large as 9% which overlaps the tiny deviations from our results (-0.5% to 3.5%) by a large margin. Note, that the fit to these data over the same temperature interval between 254 K and 363 K gives $k_1(254-363\text{ K}) = (1.35 \pm 0.12) \times 10^{-12}$

$^{12} \times \exp\{-(55 \pm 20)/T\}$, $\text{cm}^3 \text{ molecule}^{-1} \text{ s}^{-1}$. Thus all three available studies of $k_1(T)$ resulted in the same average temperature dependence of this rate constant over the common temperature range if one neglects the curvature of the Arrhenius plot. We can find the average value below room temperature, $k_1(207 - 273 \text{ K}) = (1.095 \pm 0.025) \times 10^{-12}$, $\text{cm}^3 \text{ molecule}^{-1} \text{ s}^{-1}$, which encompass all the data obtained by obtained by Papadimitriou *et al.*⁴ between 273 K and 207 K with their statistical uncertainties. Thus, the average below room temperature value of k_1 coincides with our average value shown above if one neglects the slow temperature dependence found in our study. Finally, the diamonds in Figure 1 show our unpublished results obtained for this reaction before the recent modifications and calibrations of our FP-RF apparatus. They exhibit the same temperature trend while being slightly overestimated and more scattered. The apparatus was modified to improve an accuracy of our data with a great attention paid to gas handling and all absolute calibrations. Therefore, the bold highlighted data presented in Table 1 supersede all our previous results.

The analysis of all these data allows us to conclude that the rate constant of this reaction (1) is well known and the expanded uncertainty estimated for our data is a reasonable uncertainty of this reaction rate constant.



The three-parameter modified Arrhenius dependence can be fit to the data set highlighted in Table 2:

$$k_2(220 - 370 \text{ K}) = 1.11 \times 10^{-13} \times (T / 298)^{2.03} \times \exp\{+554/T\} \text{ cm}^3 \text{ molecule}^{-1} \text{ s}^{-1} \quad (7)$$

This dependence is shown in Figure 2. It perfectly fits to all the experimental points and therefore represents $k_2(T)$ over the entire temperature range.

The detected reactive impurity in our trans-1,3,3,3-tetrafluoropropene samples was $\text{CH}\equiv\text{CCF}_3$. There are no data on OH reactivity of fluorinated propynes available. The reported rate constant for the reaction between

OH and non-substituted propyne, $\text{CH}\equiv\text{CCH}_3$ does not exceed $1\times 10^{-11} \text{ cm}^3 \text{ molecule}^{-1} \text{ s}^{-1}$. Meantime our purest sample contained only ca. 0.01% of $\text{CH}\equiv\text{CCF}_3$. Even if we accept the same rate constant for $\text{CH}\equiv\text{CCF}_3$, it cannot affect results of our measurements of k_2 . Moreover, based on reactivity trends of fluorinated propenes, it is reasonable to suggest that fluorinated propyne is even less reactive.

The only published study of this reaction was done by Sondergaard *et al.*³ who reported the rate constant determined at 296 K, $k_2(296 \text{ K}) = (9.25 \pm 1.72)\times 10^{-12} \text{ cm}^3 \text{ molecule}^{-1} \text{ s}^{-1}$. In spite of the large reported uncertainty this value definitely exceeds the result of our measurements at this temperature. The reason for this discrepancy is not clear. Both reactions (1) and (2) have similar rate constants. They were studied in the same research group, by using the same apparatus and the same relative rate technique with the same reference compounds, C_2H_4 and C_2H_2 .^{2,3} Nevertheless, $k_1(296 \text{ K})$ is only 5% smaller than our value and coincides well within the stated uncertainty. Meantime, the discrepancy in k_2 is as high as 30% so that even large reported uncertainty does not extend it down to our value. Figure 2 also shows our unpublished results obtained for this reaction before the recent modifications and calibrations of our FP-RF apparatus (open squares). They actually can be considered as independent measurements performed by using a flash photolysis – resonance fluorescence technique. They are more scattered than the present results but the agreement between these data sets is very good. Nevertheless, we believe that the accuracy of current measurements is noticeably improved and, therefore, the results presented in Table 2 supersede the previously obtained ones.

The uncertainty of OH measurements.

We increased a number of our standard temperature points where the rate constant has been measured to double-check the precision of the present OH kinetic measurements. The statistical uncertainty usually used

to present the results of such kinetic measurements can be misleading to some extent. The scattering of the original data points (the OH decay rate versus the reactant concentration plots) does not obviously obey the normal statistical distribution. Therefore, although the calculated standard errors from a least-squares fit are a measure of the scatter in the data, they probably should not be taken very strictly as the “true” confidence intervals of the normally distributed data set. This is rather the uniform and currently accepted way of data presentation and comparison. Therefore, the scattering of the finally derived average values of the rate constants around the fitted line in the Arrhenius plot can serve as a complementary evidence of the precision in addition to the reported formal statistical uncertainty of individual points. It would be the same thing in the case of normal statistical distribution of the collected data. We can imagine that this is not the case when one deals with kinetic studies of the chemical system.

The entire temperature dependence presented in Figure 2 spans 150 K along the temperature axis with ca. 9% variation of the measured rate constant, k_2 . In particular, the variation within eight points at below room temperature range of atmospheric interest is only 4.5%. Nevertheless, there is no scattering large enough to distort the obvious trend in the reactivity - the best fit curve only emphasizes the already clear dependence. The deviations of the data points in Figure 2 from the best three-parameter fit (7) are less than 0.5%. Therefore the statistical uncertainties reported in Tables 1 and 2 can be considered as reasonably small.

Finally, we summarized the reactivity of fluorinated propenes already containing the $-CF_3$ group toward OH. Table 3 shows the room temperature rate constants, $k_i(298\text{ K})$, and approximate temperature dependence, E/R , for above room temperature and below room temperature range of atmospheric interest. Note that the CF_3 substitution already dramatically decreased the reactivity of non-substituted propene by a factor of 20.¹⁷ The fluorination of olefinic carbons does not change the reactivity as much. The changes in both absolute

value of the OH reaction rate constant and its temperature trend are rather sporadic – there is no obvious correlation between the substitution site and the corresponding reactivity change. The only valuable observation one can make is that the perfluorination of olefinic carbon atoms does not change the reactivity too much in comparison with non-fluorinated molecule ($\text{CF}_2=\text{CF}-\text{CF}_3$ versus $\text{CH}_2=\text{CH}-\text{CF}_3$). The same observation was done¹ in the case of ethane fluorination ($\text{CF}_2=\text{CF}_2$ versus $\text{CH}_2=\text{CH}_2$).

IR absorption spectra

IR absorption spectra of compounds under study are presented in Figures 3, 4 and 5. The measurements were done over the pressure range of 0.2 – 3.2 kPa (1.5 Torr – 24 Torr) of $\text{CH}_2=\text{CFCF}_3$ and 0.27 – 8.5 kPa (2 Torr – 64 Torr) of $\text{CHF}=\text{CH}-\text{CF}_3$, respectively. The top panels in Figures 3 and 4 show the spectra obtained with a spectral resolution of 0.125 cm^{-1} (Boxcar apodization) to illustrate the main absorption features. The lower panels show the same spectra recorded with a spectral resolution of 0.5 cm^{-1} in Log absorption scale to illustrate smaller absorption features. IR absorption cross sections of both compounds are available in the Supporting Information and at www.nist.gov/kinetics/spectra/index.htm. Note, that these relatively large fluorinated molecules still exhibit a few sharp absorption peaks whose measured height depends on a spectral resolution and the bath gas pressure. This is rather pronounced in case of $\text{CH}_2=\text{CFCF}_3$. Thus its largest peak at 1181.5 cm^{-1} decreased by ca. 20% when recorded with the 0.5 cm^{-1} spectral resolution. The effect is even more pronounced for small longer wavelength absorption band around 615 cm^{-1} illustrated in Figure 5. Nevertheless, a few sharp absorption features do not change the integrated absorption and should not affect the estimations of global warming potentials.

Infrared absorption spectra of these compounds were recently reported in refs. 2, 3, and 4. Papadimitriou *et al.*⁴ reported integrated IR absorption band strengths of $\text{CH}_2=\text{CFCF}_3$ over a number of spectral intervals

while Nielsen *et al.*² and Sondergaard *et al.*³ reported only the total IR absorption intensity integrated over the entire range of their measurements between 650 cm⁻¹ and 2000 cm⁻¹ for both CH₂=CF₂CF₃ and CHF=CHCF₃. Table 4 presents all the available data on IR absorption intensity measurements. We accepted the wavelength intervals already chosen by Papadimitriou *et al.*⁴ for CH₂=CF₂CF₃ and somewhat arbitrary ones to present the absorption strength of CHF=CHCF₃. The last column in Table 4 shows the relative discrepancy with our results for comparison. There is a perfect agreement between the total absorption strength integrated over the entire spectral range above 650 cm⁻¹ for both compounds obtained in our work and those reported by Nielsen *et al.*² and Sondergaard *et al.*³ There is also a reasonable agreement between our data and those reported by Papadimitriou *et al.*⁴ except the longer wavelength absorption bands. The intensities of the main absorption features between 1000 cm⁻¹ and 1500 cm⁻¹ are in perfect agreement as well as that of small shorter wavelength band. In the meantime the agreement is much worse at longer wavelengths. There are two possible reasons for such increasing discrepancy. First, the IR data obtained at longer wavelength closer to the cut-off of the detector sensitivity are usually less reliable. Second, the data obtained with a cold MCT detector at longer wavelengths could be affected by the above mentioned FT-IR instrumental artifact. In our test experiments with a cold MCT detector the measured absorption cross sections were always overestimated at longer wavelengths although it was more pronounced at the highest spectral resolution.

Atmospheric implications.

The atmospheric lifetimes of CH₂=CF₂CF₃ and trans-CHF=CHCF₃ due to their reactions with tropospheric hydroxyl radicals, τ_{TFP}^{OH} , can be estimated by using the well proved simple scaling procedure which is based on results of field measurements¹⁸ and nailed by the results of thorough atmospheric modeling⁹:

$$\tau_{TFP}^{OH} = \frac{k_{MCF}(272)}{k_{TFP}(272)} \cdot \tau_{MCF}^{OH} \quad (8)$$

where τ_{TFP}^{OH} and τ_{MCF}^{OH} are the lifetimes of tetrafluoropropene under study and methyl chloroform, respectively, due to reactions with hydroxyl radicals in the troposphere only, and $k_{TFP}(272\text{ K})$ and $k_{MCF}(272\text{ K}) = 6.0 \cdot 10^{-15}\text{ cm}^3\text{molecule}^{-1}\text{s}^{-1}$ (reference 19) are the rate constants for the reactions of OH with these substances at $T=272\text{ K}$. The value of $\tau_{MCF}^{OH} = \mathbf{6.0\text{ years}}$ was obtained from the measured lifetime of MCF of 4.9 years when an ocean loss of 89 years and a stratospheric loss of 39 years were taken into account. Applying this method to the title compounds of this study yields the estimated atmospheric lifetimes of 12 days and 19 days for 2,3,3,3-tetrafluoropropene and trans-1,3,3,3-tetrafluoropropene, respectively. The lifetimes derived here are very short, much shorter than the characteristic time of mixing processes in the troposphere and hence are only crude estimates. The use of (8) is applicable for long-lived species that are well mixed throughout the troposphere. Its use for short-lived atmospheric contaminants having lifetimes shorter than the characteristic time of mixing processes in the troposphere can result in significant errors due to the large spatial gradients of their concentration in the atmosphere. For such species, equation (8) provides only rough estimates of the tropospheric lifetimes with respect to reaction with OH. The correct residence time of short-lived compounds in the atmosphere will depend on the emission location and season as well as local atmospheric conditions.^{20,21} Nevertheless, the results of these modeling studies demonstrate that such an estimation procedure gives reasonable average values^{20,21} and provides a useful scaling of the lifetimes of such compounds.

These very reactive unsaturated compounds can also react with other active components of the troposphere, Cl, O₃, NO₃. The rate constants for reactions of both compounds with Cl and O₃ were determined by Nielsen *et al.*² and Sondergaard *et al.*³ at $T = 296\text{ K}$. To the best of our knowledge, there are no data available for their reactions with NO₃. The possible effect of all these reactions on the residence time of the compounds in the atmosphere was already discussed in refs. 2, 3, and 4. It is very clear that their reactions

with tropospheric ozone are too slow to change the atmospheric lifetime. Based on the O_3 reaction rate constant $k(TFP + O_3) = 2.8 \times 10^{-21}$, $\text{cm}^3 \text{ molecule}^{-1} \text{ s}^{-1}$ reported for both compounds,^{2,3} their globally averaged atmospheric sink due to the reaction with O_3 is characterized by ca. 13 years atmospheric lifetime. Therefore even in the polluted industrial areas with the larger ozone concentrations this atmospheric sink is not comparable with OH reactions.

The situation is very different with Cl and NO_3 reactions. These reactions can significantly change the atmospheric lifetime of the compounds under study especially in some locations and periods of time. Unfortunately, in great contrast with OH, these changes are much more difficult to quantify presently. The rate constants of the reactions between tetrafluoropropenes under study and Cl are much larger than those with OH.^{2,3} On the other hand, the concentration of Cl atoms in the atmosphere is much smaller than the OH concentration, although it is not well established and large fluctuations are expected in some regions of the marine boundary layer.²² Some estimations allow it to be as large as 10^4 molecule/ cm^3 in the free troposphere.^{22,23} Assuming such a globally average concentration of chlorine atoms we can estimate the atmospheric lifetimes due to reactions with Cl only to be as short as 16 days and 25 days for $\text{CH}_2=\text{CFCF}_3$ and trans-CHF=CHCF₃, respectively. These lifetimes are roughly the same as OH reaction related lifetimes estimated above. If we accept these Cl reaction related lifetimes, the global atmospheric lifetimes of $\text{CH}_2=\text{CFCF}_3$ and trans-CHF=CHCF₃ will become as short as 7 days and 11 days, respectively. Again, these estimations are based on the assumption of the global average concentration of atmospheric Cl as large as 10^4 molecule/ cm^3 which is not established well enough to make definite conclusions.

It is an even worse situation with estimating the possible effect of NO_3 reactions as the atmospheric sink: neither NO_3 reaction rate constants nor its atmospheric concentration are known. To the best of our

knowledge, there are no available data on the reactivity of the title compounds toward NO_3 . The available rate constants at $T = 298 \text{ K}$ for reactions of NO_3 with analogous molecules are 9.5, 3.8, <3, and 3 for $\text{CH}_2=\text{CHCH}_3$,²⁴ $\text{CH}_2=\text{CHCH}_2\text{F}$,²⁵ $\text{CF}_2=\text{CFCF}_3$,²⁶ and $\text{CF}_2=\text{CF}_2$,²⁷ respectively (units are $10^{-15} \text{ cm}^3 \text{ molecule}^{-1} \text{ s}^{-1}$). Therefore one can make rough estimations with $3 \times 10^{-15} \text{ cm}^3 \text{ molecule}^{-1} \text{ s}^{-1}$ while keeping in mind that it can be as large as $1 \times 10^{-14} \text{ cm}^3 \text{ molecule}^{-1} \text{ s}^{-1}$. NO_3 appears in the troposphere as a result of a number of fast photochemical processes. Its concentration is low during daylight hours and generally increases after sunset. The atmospheric concentration of NO_3 in the moderately polluted lower troposphere can be 10-20 pptv;^{28,29} it can be even larger in the polluted areas. It is much lower over marine areas because of the low NO_2 concentrations.^{30,31} Based on the above, the atmospheric lifetime of the title compounds due to their reactions with NO_3 can be roughly estimated to be longer than 1-2 months. Note that this is a very uncertain estimation which is based on an assumed reaction rate constant and a very uncertain NO_3 concentration, which is probably the greatest contributor to the overall uncertainty. This estimation is only to illustrate that the reaction with NO_3 can give small although noticeable corrections to OH dictated atmospheric lifetime over the majority of relatively unpolluted areas. This correction can become comparable with τ_{TFP}^{OH} in the highly NO_2 polluted areas.

The above estimations show that the reactions with atmospheric NO_3 and especially with Cl can make the atmospheric lifetimes of the title compounds shorter. However, these corrections are highly uncertain in contrast with well developed and proven estimations of the lifetime dictated by the compound's reaction with the atmospheric hydroxyl radicals. Therefore, we will use τ_{TFP}^{OH} when estimating global warming potentials of the compounds while keeping in mind that it represents only an upper limit of the atmospheric lifetime.

We can make simplified estimations of global warming potentials of 2,3,3,3-tetrafluoropropene and trans-1,3,3,3-tetrafluoropropene by combining their estimated atmospheric lifetimes, measured IR absorption spectra and the measured spectrum of Earth's outgoing radiation.^{32,33,34} We first calculated the time-dependent hydrocarbon global warming potentials with CFC-11 as a reference compound, $HGWP_{TFP}(t)$. This referencing takes advantage of the fact that the time response functions for both the tetrafluoropropene under estimation and the CFC-11 reference can be approximated as exponential decays. Hence, $HGWP_{TFP}(t)$ can be calculated as follows:^{32,35}

$$\begin{aligned}
 HGWP_{TFP}(t) &= RRF_{TFP}^{CFC-11} \frac{M_{CFC-11}}{M_{TFP}} \frac{\int_0^t \exp\{-t/\tau_{TFP}\} dt}{\int_0^t \exp\{-t/\tau_{CFC-11}\} dt} = \\
 &= RRF_{TFP}^{CFC-11} \times \frac{M_{CFC-11}}{M_{RH}} \times \frac{\tau_{TFP}}{\tau_{CFC-11}} \times \frac{1 - \exp\{-t/\tau_{TFP}\}}{1 - \exp\{-t/\tau_{CFC-11}\}}
 \end{aligned} \tag{9}$$

Here M_{CFC-11} and M_{TFP} are molecular masses of CFC-11 and tetrafluoropropene, respectively and RRF_{TFP}^{CFC-11} is the relative radiative forcings (using CFC-11 as a reference) for tetrafluoropropene under study:

$$RRF_{TFP}^{CFC-11} = \frac{\int_{\nu_1}^{\nu_2} \sigma_{TFP}(\nu) \times \Phi(\nu) d\nu}{\int_{\nu_1}^{\nu_2} \sigma_{CFC-11}(\nu) \times \Phi(\nu) d\nu} \tag{10}$$

where ν_1 and ν_2 are the integration limits and $\Phi(\nu)$ is the intensity of outgoing Earth's radiation - experimentally measured spectrum of outgoing Earth's radiation obtained from the NIMBUS-4 satellite at a latitude of $15^\circ N$ ³⁶ in our calculations. Nielsen *et al.*² and Sondergaard *et al.*³ used the similar approach suggested by Pinnock *et al.*³³ with model calculated irradiance at the tropopause. Then we used the global warming potential of CFC-11 referenced to CO₂ (GWP_{CFC-11}) calculated using a radiative transfer model of the atmosphere and accepted in the 2006 International Scientific Assessment of Ozone Depletion³⁷ to obtain global warming potentials of these tetrafluoropropenes over various time horizons:

$$GWP_{TFP}(t) = RRF_{TFP}^{CFC-11} \times GWP_{CFC-11}(t) \tag{11}$$

Thus calculated GWPs are presented in Table 5 for time horizons of 20 years, 100 years, and 500 years.

Note that this estimation procedure is not valid for gases with very short atmospheric lifetimes, since they do not have a uniform mixing ratio either vertically in the upper troposphere and tropopause region or geographically with latitude as does the CFC-11 reference compound. Meantime, absorption of the Earth's outgoing radiation takes place in the upper part of the troposphere at colder temperature. In addition, the residence time of the compound in the atmosphere can be shorter than the OH reaction directed one, τ_{TFP}^{OH} , due to reactions with atmospheric Cl and NO₃. Therefore, these estimations under assumption of the well mixed atmosphere result in an overestimation of GWPs of short-lived compounds. Nevertheless, they provide a useful scaling of GWPs of such very short lived compounds in the absence of any other simple indices.

Acknowledgment

Authors thank Dr. Jay H. Hendricks for the timely manometer calibration to the NIST pressure standard and Dr. Anatoly Tereza for the help with other calibrations.

This work was supported by the Upper Atmosphere Research Program of the National Aeronautics and Space Administration and NIST Measurement Services Advisory Group. VLO acknowledges the support of NATO CLG Program, Grant ESP.EAP.CLG.983035.

Supporting Information Available:

The IR absorption cross sections of CH₂=CFCF₃ and *trans*-CHF=CHCF₃ are presented in Tables 5 and 6.

This material is available free of charge via the Internet at <http://pubs.acs.org>.

Table 1 Rate Constants Measured in the Present Work for the Reaction of OH with CH₂=CF-CF₃ (2,3,3,3-tetrafluoropropene).^a

<i>T</i> , K	<i>k_f</i> (<i>T</i>) × 10 ¹² , cm ³ molecule ⁻¹ s ⁻¹	[CH ₂ =CF-CF ₃], 10 ¹³ molecule/cm ³	Test experiments conditions
220	1.079 ± 0.011	1.6 – 16.7	
230	1.081 ± 0.008	2.4 – 31.6	
	1.108 ± 0.012	2.7 – 16.7	100 Torr
	1.018 ± 0.024	2.7 – 22.6	200 Torr
	1.013 ± 0.066	1.7 – 21.3	300 Torr
250	1.089 ± 0.011	1.4 – 16.2	
272	1.091 ± 0.012	2.0 – 13.5	
298	1.096 ± 0.007	1.8 – 24.4	
	1.103 ± 0.009	2.0 – 20.6	100 Torr
	1.097 ± 0.022	2.0 – 17.1	200 Torr
	<i>1.087 ± 0.011</i>	<i>2.3 – 19.3</i>	<i>Total Flow Rate 25%</i>
	<i>1.100 ± 0.009</i>	<i>1.2 – 12.1</i>	<i>Total Flow Rate 200%</i>
	<i>1.100 ± 0.020</i>	<i>2.0 – 16.3</i>	<i>0.1% mixture in the bulb</i>
	<i>1.085 ± 0.021</i>	<i>2.2 – 27.7</i>	<i>10% mixture in the bulb</i>
313	1.109 ± 0.011	1.7 – 23.3	
330	1.123 ± 0.016	1.7 – 15.5	
350	1.140 ± 0.010	1.6 – 20.8	
370	1.166 ± 0.012	1.5 – 19.9	

^a The uncertainties are two Standard Errors from the least-squares fit of a straight line to the measured OH decay rates versus the reactant concentrations. They do not include the estimated instrumental/systematic uncertainty of ca. 2%.

Table 2. Rate Constants Measured in the Present Work for the Reaction of OH with *trans*-CHF=CH-CF₃ (trans-1,3,3,3-tetrafluoropropene).

<i>T</i> , K	$k_2(T) \times 10^{13}$, cm ³ molecule ⁻¹ s ⁻¹	[CHF=CHCF ₃], 10 ¹³ molecule/cm ³	Test experiments conditions
220	7.39 ± 0.08	2.6 – 30.0	
230	7.29 ± 0.06	2.5 – 33.0	
240	7.19 ± 0.16	2.4 – 18.4	
250	7.09 ± 0.07	4.5 – 30.6	
260	7.11 ± 0.09	4.3 – 25.2	
272	7.03 ± 0.09	2.1 – 39.8	
285	7.05 ± 0.12	4.0 – 38.0	
298	7.11 ± 0.05	2.0 – 60.0	
	6.89 ± 0.31	3.5 – 22.7	200 Torr
	7.18 ± 0.14	3.5 – 34.8	3% mixture
	7.30 ± 0.28	3.9 – 34.2	0.3% mixture
	7.01 ± 0.27	14.0 – 43.0	100% mixture
313	7.19 ± 0.10	3.6 – 34.6	
330	7.37 ± 0.11	3.4 – 32.9	
350	7.49 ± 0.08	3.2 – 31.0	
370	7.69 ± 0.07	3.1 – 29.3	

^a The uncertainties are two Standard Errors from the least-squares fit of a straight line to the measured OH decay rates versus the reactant concentrations. They do not include the estimated instrumental/systematic uncertainty of ca. 2%.

Table 3. Summary of OH Reactivity of Fluorinated Propenes Containing $-\text{CF}_3$.

Fluorinated Propene	$k_i(298\text{ K}) \times 10^{12}$, $\text{cm}^3 \text{molecule}^{-1} \text{s}^{-1}$	E/R (T < 298 K), K	E/R (298 K < T < 370 K), K
$\text{CH}_2=\text{CH}-\text{CF}_3$	1.5	-180	-180
$\text{CH}_2=\text{CF}-\text{CF}_3$	1.1	+13	+90
$\text{CHF}=\text{CH}-\text{CF}_3$	0.7	-40	+120
$\text{CHF}=\text{CF}-\text{CF}_3$	1.3	-170	+20
$\text{CF}_2=\text{CF}-\text{CF}_3$	2.2	-430	-410

Table 4. Integrated infrared absorption band strengths obtained for CH₂=CF-CF₃ and CHF=CH-CF₃ (10⁻¹⁷ cm²molecule⁻¹cm⁻¹).

Integration Range, cm ⁻¹	This work ^a	Nielsen et al., 2007 ^b	Søndergaard et al., 2007 ^b	Papadimitriou et al., 2008 ^c (presented)	Papadimitriou et al., 2008 ^c (from ESM)	Deviation from this work, %
CH₂=CF-CF₃						
540 - 655	0.4830			0.47 ± 0.05	0.5657	+17.1
850 - 920	0.5910			0.63 ± 0.01	0.6746	+14.1
920 - 1000	0.3749			0.35 ± 0.01	0.3959	+5.6
1065 - 1296	12.039			12.0 ± 0.02	12.244	+1.7
1307 - 1498	2.942			2.79 ± 0.02	2.9478	0.0
1580 - 1810	0.7826			0.66 ± 0.01	0.7737	-1.2
800 - 2000	16.90		16.3 (± 5%)			-0.7
CHF=CH-CF₃						
660 - 725	0.436					
780 - 980	1.222					
1050 - 1128	5.042					
1128 - 1212	5.919					
1212 - 1295	2.025					
1295 - 1370	2.185					
1590 - 1820	2.534					
650 - 2000	19.59	19.4 (±5%)				-1.0

^a The overall expanded uncertainty is estimated to be ca. 2% (see the text). T = 298 K.

^b Authors report 5% as the total expanded uncertainty which includes the estimated systematic uncertainty of measurements. T = 296 K

^c The quoted uncertainties are two standard error of the from the statistical treatment of the data only. T = 296 K.

Table 5. Atmospheric lifetimes of tetrafluoropropenes due to reactions with OH their and GWPs.

Molecule	Atmospheric lifetime, days	GWPs at time horizons:		
		20 years	100 years	500 years
CH ₂ =CF ₂ CF ₃	12	15.5	4.4	1.3
CHF=CHCF ₃	19	26.6	7.5	2.3

Figure captions.

Figure 1 Results of the rate constant measurements for the reaction between OH and $\text{CH}_2=\text{CFCF}_3$ - $k_1(T)$.

• - this work; □ - Papadimitriou *et al.*,⁴ Δ - Nielsen *et al.*,² o - our measurements before apparatus modification/calibration, ◇ - Orkin *et al.*¹. Uncertainties shown for our present data and data by Papadimitriou *et al.*, are two standards errors from the fit while uncertainty from Nielsen *et al.*, were chosen to encompass the extremes of their data. The dashed line is the best fit to our data with a three-parameter modified Arrhenius expression; the solid line is $k_1(T) = 1.146 \times 10^{13} \times \exp\{-13/T\}$.

Figure 2 Results of the rate constant measurements for the reaction between OH and *trans*- $\text{CHF}=\text{CHCF}_3$ - $k_2(T)$.

• - this work; Δ - Sondergaard *et al.*,³ □ - our measurements before apparatus modification/calibration. Uncertainties shown for our data are two standards errors from the fit while uncertainty from Sondergaard *et al.* were chosen to encompass the extremes of their data. The dashed line is the best fit to our data with a three-parameter modified Arrhenius expression $k_2(T) = 1.1 \times 10^{-13} \times (T/298)^{2.03} \times \exp\{-13/T\}$.

Figure 3 IR absorption spectrum of $\text{CH}_2=\text{CFCF}_3$ obtained with a spectral resolution of 0.125 cm^{-1} (top panel) and 0.5 cm^{-1} (lower panel). The later is shown in Log scale to visualize smaller absorption features.

Figure 4 IR absorption spectrum of *trans*- $\text{CHF}=\text{CHCF}_3$ obtained with a spectral resolution of 0.125 cm^{-1} (top panel) and 0.5 cm^{-1} (lower panel). The later is shown in Log scale to visualize smaller absorption features.

Figure 5 IR absorption band of $\text{CH}_2=\text{CFCF}_3$ between 560 cm^{-1} and 640 cm^{-1} obtained with a spectral resolution of 0.125 cm^{-1} (top panel) and 0.5 cm^{-1} (lower panel).

References:

- (1) Orkin, V. L.; Huie, R. E.; Kurylo, M. J. *J. Phys. Chem. A*, **1997**, *101*, 9118-9124.
- (2) Nielsen, O. J.; Javadi, M. S.; Andersen, M. P. S.; Hurley, M. D.; Wallington, T. J.; Singh, R. *Chemical Physics Letters*, **2007**, *439*, 18–22.
- (3) Søndergaard, R.; Nielsen, O. J.; Hurley, M. D.; Wallington, T. J.; Singh, R. *Chemical Physics Letters*, **2007**, *443*, 199–204.
- (4) Papadimitriou, V. C.; Talukdar, R. K.; Portmann, R. W.; Ravishankara A. R.; Burkholder, J. B. *Phys. Chem. Chem. Phys.* **2008**, *10*, 808–820.
- (5) Certain commercial equipment, instruments, or materials are identified in this article in order to adequately specify the experimental procedure. Such identification does not imply recognition or endorsement by the National Institute of Standards and Technology, nor does it imply that the material or equipment identified are necessarily the best available for the purpose.
- (6) Kurylo, M. J.; Cornett, K. D.; Murphy, J. L. *J. Geophys. Res.* **1982**, *87*, 3081-3085.
- (7) Orkin, V. L.; Huie, R. E.; Kurylo, M. J. *J. Phys. Chem.* **1996**, *100*, 8907-8912.
- (8) Orkin, V. L.; Khamaganov, V. G.; Guschin, A. G.; Huie, R. E.; Kurylo, M. J. *J. Phys. Chem.* **1997**, *101*, 174-178.
- (9) Spivakovsky, C. M.; Logan, J. A.; Montzka, S. A.; Balkanski, Y. J.; Foreman-Fowler, M.; Jones, D. B. A.; Horowitz, L. W.; Fusco, A. C.; Brenninkmeijer, C. A. M.; Prather, M. J.; Wofsy, S. C.; McElroy, M. B. *J. Geophys. Res.* **2000**, *105*, 8931-8980.
- (10) J. W. Johns, J. W. *Technical Digest Series, Optical Society of America*, **1995**, *4*, Washington, D.C.
- (11) Giver, L. P.; Chackerian, Jr., C.; Spencer, M. N. *Technical Digest, Optical Society of America*, **1992**, *21*, Washington, D.C.

-
- (12) Sharpe, S. W.; Johnson, T. J.; Sams, R. L.; Chu, P. M.; Rhoderick, G. C.; Johnson, P. A. *Applied Spectroscopy*, **2004**, *58*, 1452-1461.
- (13) Powell, R. L.; Hall, W. J.; Hyink, Jr., C. H.; Sparks, L. L.; Burns, G. W.; Scroger, M. G.; Plumb, H. H. **1974**, NBS Monograph 125.
- (14) Kurylo, M. J. and Orkin, V. L. *Chem. Rev.* **2003**, *103*, 5049-5076.
- (15) Orkin, V. L.; Huie, R. E.; Kurylo, M. J. *J. Phys. Chem.* **1997**, *101*, 9118-9124.
- (16) Nielsen, O. J.; Javadi, M. S.; Sulbaek Andersen M. P.; Hurley, M. D.; Wallington T. J.; Singh R. 2007, *Chemical Physics Letters*, **2007**, *439*, 18–22.
- (17) Atkinson, R.; Baulch, D. L.; Cox, R. A.; Hampson, R. F., Jr.; Kerr, J. A.; Rossi, M. J.; Troe, J. *J. Phys. Chem. Ref. Data* **1997**, *26*, 521 – 1011.
- (18) Prinn, R. G.; Huang, J.; Weiss, R. F.; Cunnold, D. M.; Fraser, P. J.; Simmonds, P. G.; McCulloch, A.; Harth, C.; Salameh, P.; O'Doherty, S.; Wang, R. H. J.; Porter, L.; Miller, B. R. *Science* **2001**, *292*, 1882.
- (19) Sander, S. P.; Friedl, R. R.; Golden, D. M.; Kurylo, M. J.; Moortgat, G. K.; Keller-Rudek, H.; Wine, P. H.; Ravishankara, A. R.; Kolb, C. E.; Molina, M. J.; Finlayson-Pitts, B. J.; Huie, R. E.; Orkin, V. L.; *Chemical Kinetics and Photochemical Data for Use in Atmospheric Studies, Evaluation No. 15*; JPL Publication 06-2; Jet Propulsion Laboratory, California Institute of Technology: Pasadena, CA 2006.
- (20) Bridgeman, C. H.; Pyle, J. A.; Shallcross, D.E. *J. Geophys. Res.* **2000** *105*, 26493.
- (21) Wuebbles, D. J.; Patten, K. O.; Johnson, M. T.; Kotamarthi, R. *J. Geophys. Res.* **2001**, *106*, 14551.
- (22) Spicer, C. W.; Chapman, E. G.; Finlayson-Pitts, B. J.; Plastridge, R. A.; Hubbe, J. M.; Fast, J. D.; Berkowitz, C. M. *Nature* **1998**, *394*, 353–356.
- (23) Platt, U.; Allen, W.; Lowe, D. *Atmos. Chem. Phys.* **2004**, *4*, 2283–2300.

-
- (24) Atkinson, R.; Baulch, D. L.; Cox, R. A.; Crowley, J. N.; Hampson, R. F, Jr.; Kerr, J. A.; Rossi, M. J.; Troe, J. Summary of Evaluated Kinetic and Photochemical Data for Atmospheric Chemistry **2001**, 1–56.
- (25) Martinez, E.; Cabanas, B.; Aranda, A.; Martin, P.; Salgado, S. *Int. J. Chem. Kinet.* **1997**, *29*, 927–932.
- (26) Acerboni, G.; Beukes, J. A.; Jensen, N. R.; Hjorth, J.; Myhre, G.; Nielsen, C. J.; Sundet, J. K. *Atmos. Environ.* **2001**, *35*, 4113-4123.
- (27) Acerboni, G.; Jensen, N. R.; Rindone, B.; Hjorth, J. *Chem. Phys. Lett.* **1999**, *309*, 364 – 368.
- (28) Wayne, R.P. (ed.) *Atmos. Environ.* **1991**, *25*, 1-203.
- (29) Atkinson R. *J Phys Chem Ref. Data* **1991**, *20*, 459-507.
- (30) Noxon J. F. *J Geophys Res* **1983**, *88*, 11017-11021.
- (31) Winer A. M.; Atkinson R.; Pitts J. N. Jr. *Science* **1984**, *224*, 156-159.
- (32) Orkin, V. L.; Khamaganov, V. G.; Guschin, A. G.; Kasimovskaya, E. E.; Larin, I. K. Development of Atmospheric Characteristics of Chlorine-Free Alternative Fluorocarbons. Report on R-134a and E-143a, Report ORNL/Sub/86X-SL103V prepared for the Oak Ridge National Laboratory (1993).
- (33) Pinnock, S.; Hurley, M. D.; Shine, K. P.; Wallington, T. J.; Smyth, T. J. *J. Geophys. Res.* **1995**, *100*, 23,227-23,238.
- (34) Orkin, V. L.; Guschin, A. G.; Larin, I. K.; Huie, R. E.; Kurylo, M. J. *J. Photochem. Photobiol. A* **2003**, *157*, 211.
- (35) Roehl, C. M.; Boglu, D.; Brühl, C.; Moortgat, G. K. *Geophys. Res. Lett.* **1995**, *22*, 815.
- (36) Kunde, V. G.; Conrath, B. J.; Hanel, R. A.; Maguire, W. C.; Prabhakara, C.; Salomonson, V. V. *J. Geophys. Res.* **1974**, *79*, 777-784.

-
- (37) World Meteorological Organization. Global Ozone Research and Monitoring Project - Report No. 50
Scientific Assessment of Ozone Depletion: 2006, 572 pp., Geneva, Switzerland, 2007.

Figure 1, Orkin et al., 2008

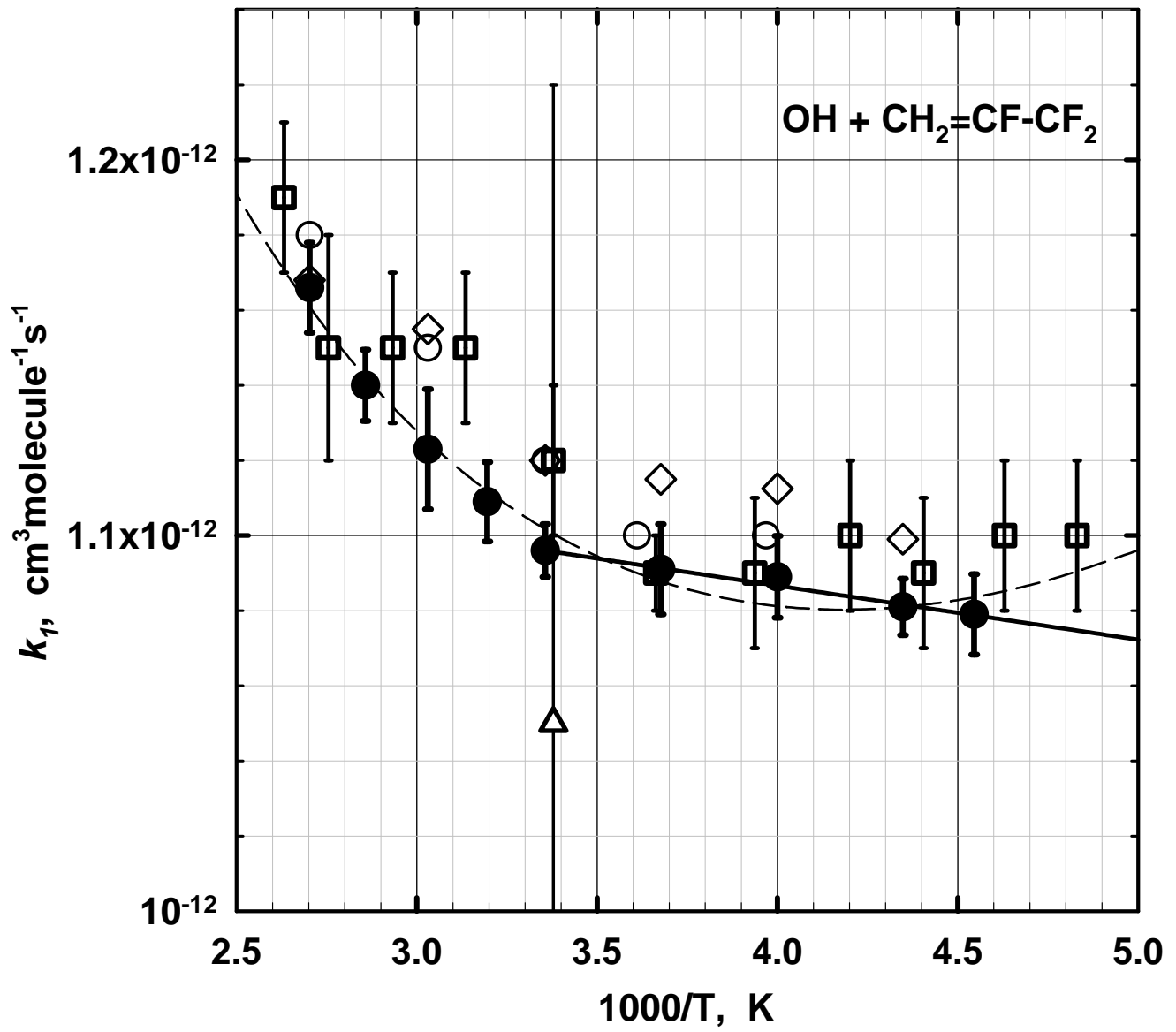


Figure 2, Orkin et al., 2008

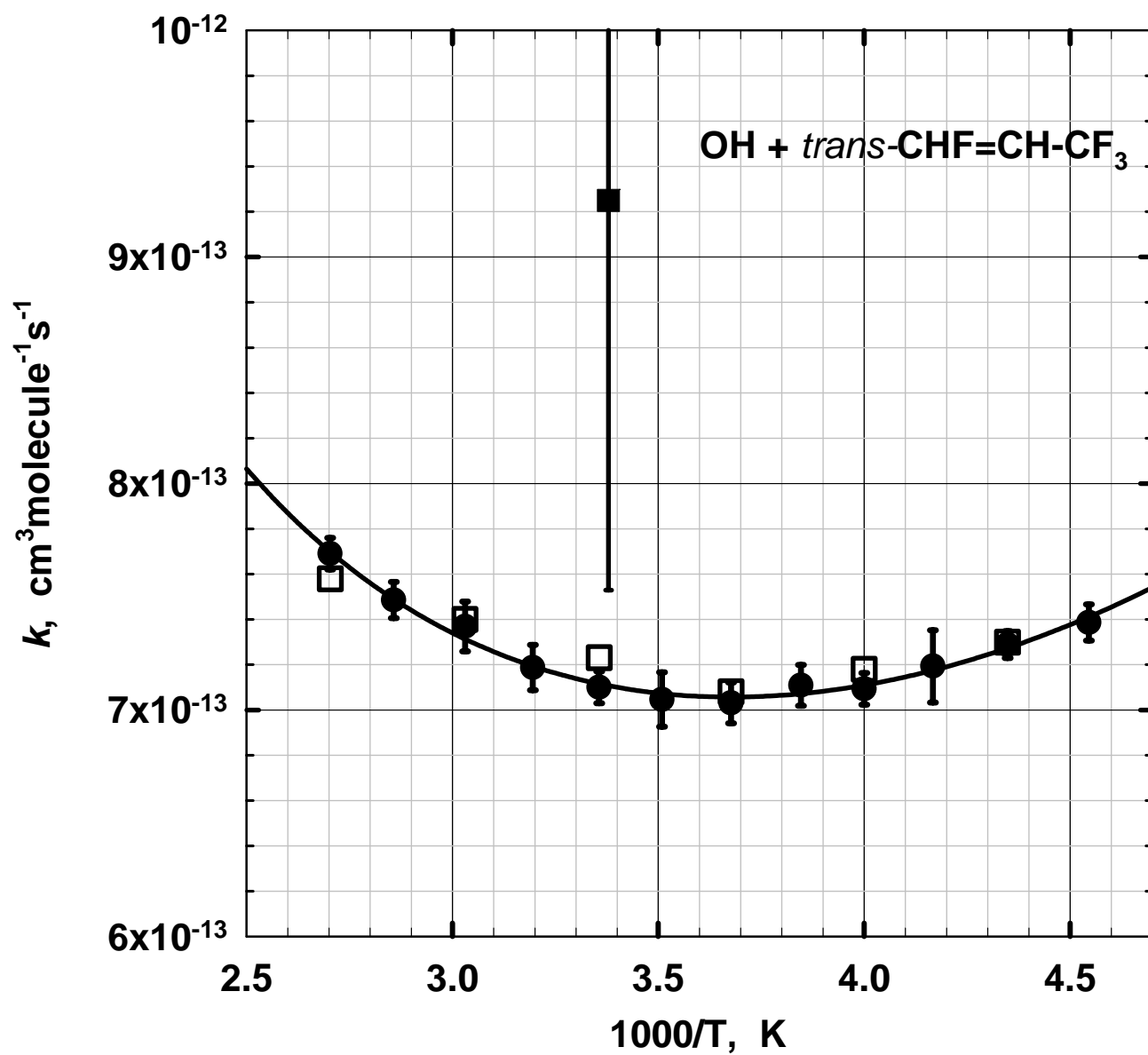


Figure 3, Orkin et al., 2008

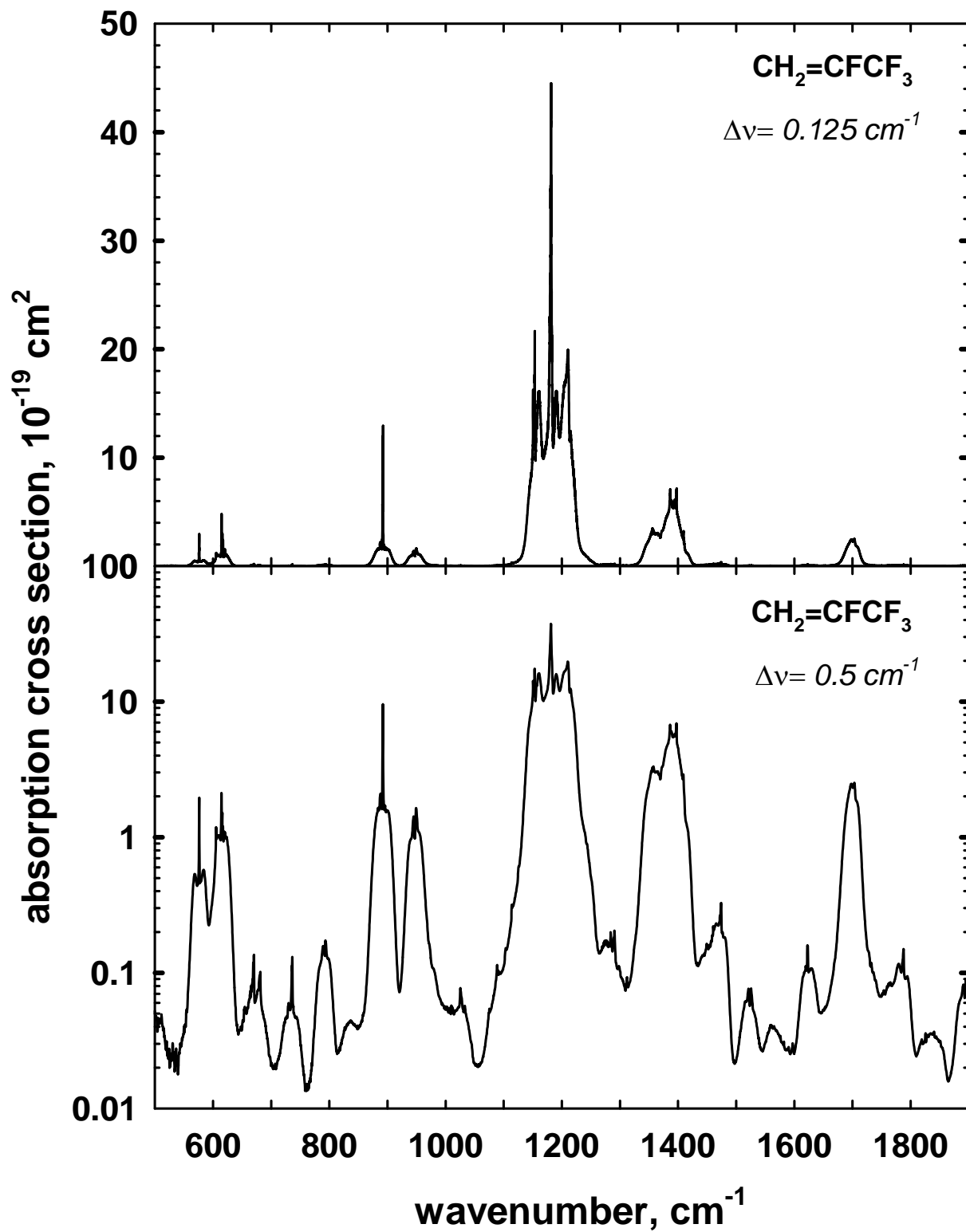


Figure 4, Orkin et al., 2008

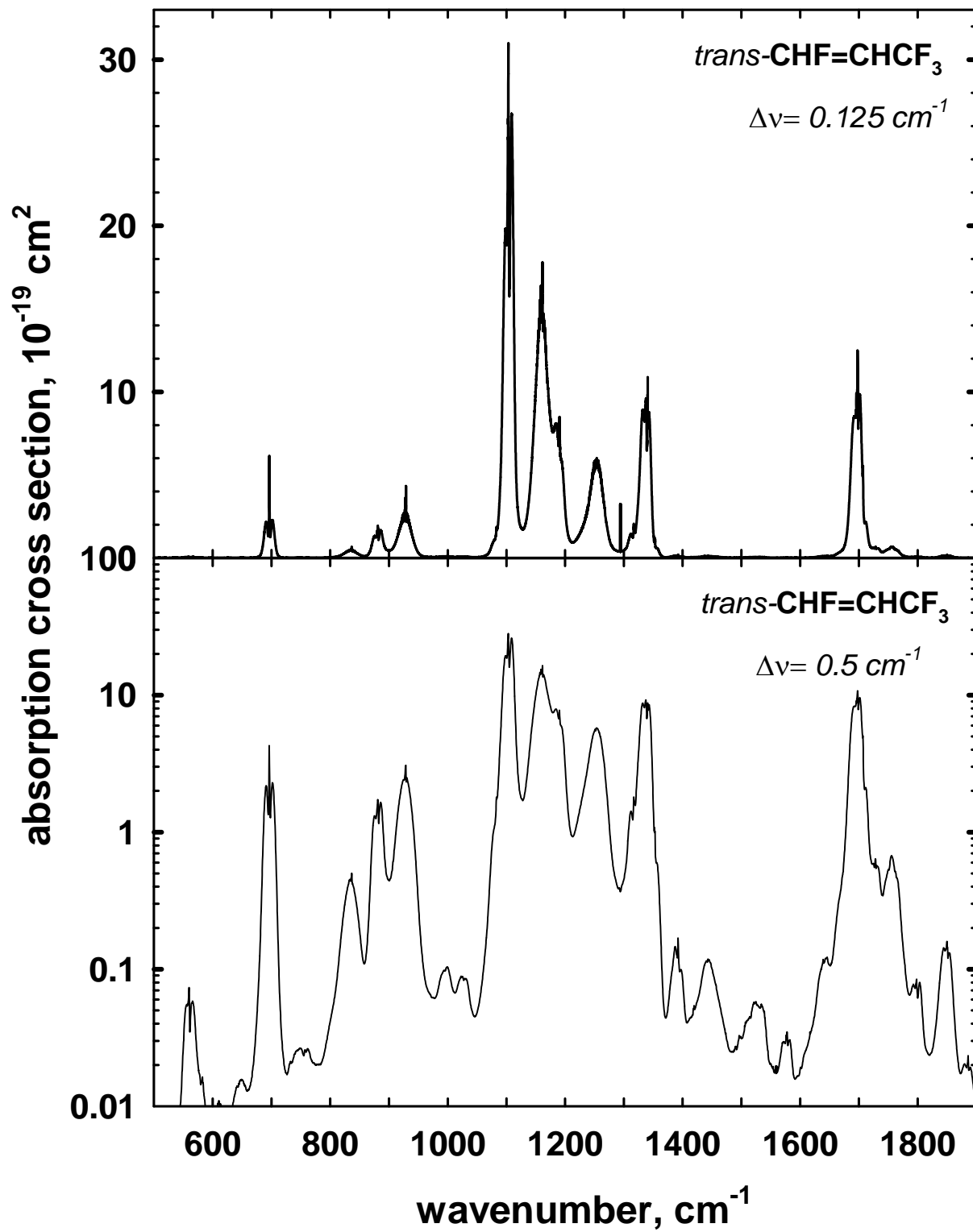


Figure 5, Orkin et al., 2008

